Research paper

Dynamic fracture process analysis in rock-like materials for axisymmetric problem

Hakman Kim*, Daisuke Fukuda**†, Junko Ikezawa*, Kazuma Moriya*, Sang Ho Cho***, and Katsuhiko Kaneko**

*Graduate School of Engineering, Hokkaido University, Kita 13 Nishi 8, Kita-ku, Sapporo, Hokkaido 060-8628, Japan
Phone : +81-11-706-6325

**Faculty of Engineering, Hokkaido University, Kita 13 Nishi 8, Kita-ku, Sapporo, Hokkaido 060-8628, Japan
Phone : +81-11-706-6322
†Corresponding address : daichang@geo-er.eng.hokudai.ac.jp

***Department of Mineral Resources & Energy Engineering, Chonbuk National University 664-141 Ga Deokjin-Dong, Jeonju-City, Chonlabuk-Do, 561-756, South Korea

Received : October 31, 2012 Accepted : November 25, 2013

Abstract

Dynamic fracture mechanics in rock-like materials such as concrete and rocks due to application of blast-loads is quite important engineering topic because blasting is cost-effective high-speed fragmentation technique. To understand the mechanism in detail, reasonable numerical simulation method to analyze the 3-D complicated fracture process is required. In the application of detonation or deflagration of explosives, cylindrical charge is often adopted and axisymmetric condition can be applicable to this case, reducing the 3-D problem to 2-D one. Thus we developed a new method to conduct 3-D fracture simulation for rock-like materials based on the finite element method under the axisymmetric condition. We explained the methodology in detail. We showed the applicability of the proposed method to the evaluation of the fracture process for the class of problem where the axisymmetry holds.

Keywords : dynamic fracture process analysis, rock-like material, finite element method, axisymmetric problem, cohesive law

1. Introduction

Understanding fracture mechanism in rock-like materials such as concrete and rocks due to application of rapid loads is of engineering importance in such as blasting and other high-speed fragmentation techniques. In these techniques, control of crack propagation direction and the resultant fracture pattern is often required for design optimization. For this purpose, the Dynamic Fracture Process Analysis (DFPA) for 2 dimensional (2-D) problem has been proposed and applied to the simulation of blasting. However, to understand fracture pattern and detailed knowledge of 3 dimensional (3-D) fracture process for each technique is required.

In case of utilizing detonation or deflagration of explosives for fragmentation of rock-like materials, cylindrical charge is frequently applied[1] and corresponding geometrical representation of the problem can be considered as axisymmetric. Thus 3-D elastodynamic problem can be treated as 2 dimensional problem under the axisymmetry[1].

In this study, we developed a new numerical simulation method to conduct DFPA based on finite element method (FEM) under elastodynamic axisymmetric condition in which crack initiation, propagation and coalescence in rock-like materials are considered[2,3]. This paper describes the methodology and investigates the applicability of the proposed method.

2. Numerical simulation method (DFPA)

2.1 FEM for axisymmetric problem

In this paper, we considered a cylindrical charge shown in Figure 1 (a). The figure is shown by cylindrical

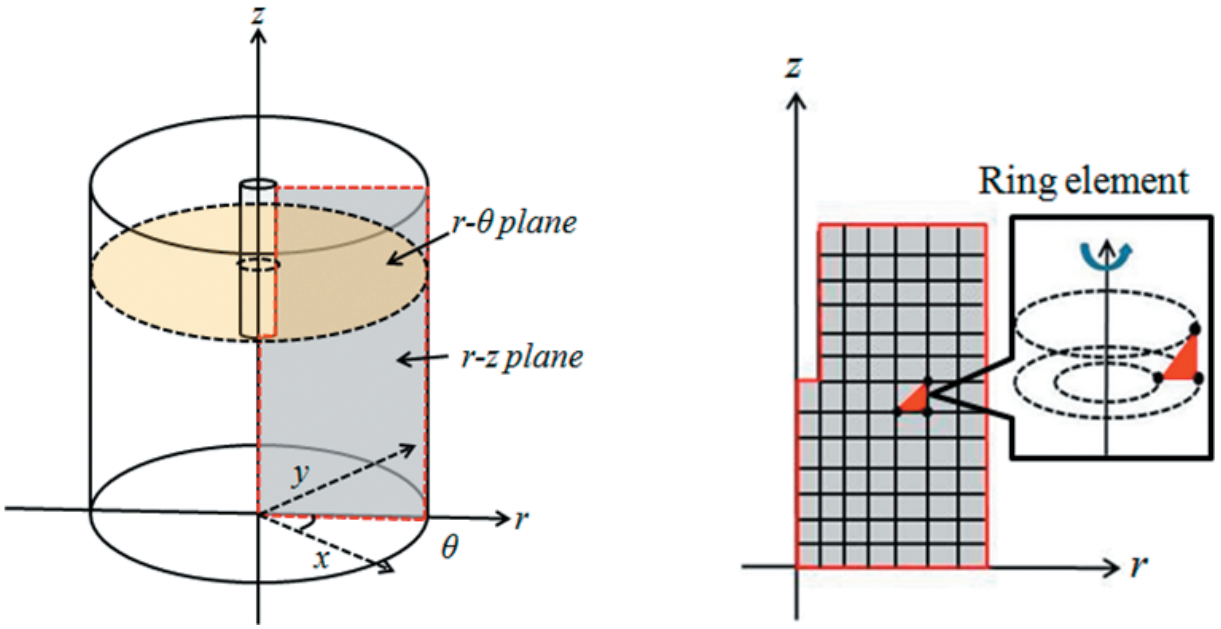

(a) Axisymmetry with respect to $z-$axis (b) Finite element discretization

Figure 1 Treatment of axisymmetric problem in FEM.

coordinate (r,θ,z) where z coincides with the axial direction of the charge hole, and r and θ are polar coordinates at the cross section perpendicular to the z axis. If the domain of interest has axisymmetric property with respect to z axis, u_θ in the displacement field (u_r,u_θ,u_z) becomes zero. Thus, only u_r and u_z need to be considered. By discretizing the domain of interest by FEM based on triangular ring elements, it can be reduced to the FEM mesh shown in Figure 1(b).

Coordinates (r,z), displacements (u_r,u_z), velocities $(\dot{u}_r,\dot{u}_z)$ and accelerations $(\ddot{u}_r,\ddot{u}_z)$ are interpolated through isoparametric mapping to parent coordinate (ξ,η) where the nodal variables are expressed as the multiplication of shape functions $N_I(\xi,\eta)$[4] for node I from 1 to 3, by nodal coordinates (r_I,z_I), nodal displacements (u_{rI},u_{zI}), nodal velocities $(\dot{u}_{rI},\dot{u}_{zI})$ and nodal accelerations $(\ddot{u}_{rI},\ddot{u}_{zI})$, respectively. As stress and strain measures, infinitesimal strain $\{\varepsilon_k\}=\{\varepsilon_r,\varepsilon_z,\varepsilon_\theta,2\varepsilon_{rz}\}(k=1,\cdots,4)$ and Cauchy stress $\{\sigma_k\}=\{\sigma_r,\sigma_z,\sigma_\theta,\sigma_{rz}\}(k=1,\cdots,4)$ are used. The relationship between $\{\varepsilon_k\}$ and (u_{rI},u_{zI}) is given by :

$$\{\varepsilon_k\}=\begin{Bmatrix}\varepsilon_r(r,z,t)\\ \varepsilon_z(r,z,t)\\ \varepsilon_\theta(r,z,t)\\ 2\varepsilon_{rz}(r,z,t)\end{Bmatrix}=\sum_{I=1}^{3}\begin{bmatrix}\frac{\partial N_I}{\partial r} & 0\\ 0 & \frac{\partial N_I}{\partial z}\\ \frac{N_I}{r} & 0\\ \frac{\partial N_I}{\partial z} & \frac{\partial N_I}{\partial r}\end{bmatrix}\begin{Bmatrix}u_{rI}\\ u_{zI}\end{Bmatrix}=\sum_{I=1}^{3}\sum_{j=1}^{2}(B_I)_{kj}\cdot u_{jI}$$

for $k=1,\cdots,4$ (1)

where $j=1$ and 2 indicate r and z directions, respectively. For the constitutive relation between stress and strain before crack initiation, the isotropic linear elastic behavior is assumed, which gives :

$$\{\sigma_k\}=\{D_{kl}\varepsilon_l\}\,\text{for}\,(k\,\text{and}\,l=1,\cdots,4) \tag{2}$$

where, by denoting Young's modulus and Poisson's ratio by E and ν, respectively, D_{kl} is given by $D_{11}=D_{22}=D_{33}=E(1-\nu)/\{(1+\nu)(1+2\nu)\}$, $D_{21}=D_{12}=D_{31}=D_{13}=E\nu/(1+\nu)/(1+2\nu)$, $D_{44}=E/(1+\nu)/2$ and otherwise $D_{kl}=0$.

The spatially discretized form of equation of motion is given as :

$$\sum_{I=1}^{3}\left(\sum_{J=1}^{3}\sum_{j=1}^{2}(M_{IJij}(t)\ddot{u}_{jJ}(t))+f_{Ii}^{\text{int}}(t)\right)=\sum_{I=1}^{3}\left(f_{Ii}^{\text{ext}}(t)\right)\ \text{for}\ i=1,2 \tag{3}$$

where M_{IJij}, f_{iI}^{int} and f_{iI}^{ext} are indicial notation of mass matrix, internal and external nodal forces, respectively, each of which is given by following equations :

$$M_{IJij}(t)=2\pi\delta_{ij}\int\!\!\int_S \rho N_I N_J r\,dr\,dz \ \text{for}\ I\,\text{and}\,J=1,\cdots,3\ \text{and}\ i\,\text{and}\,j=1,2 \tag{4}$$

$$f_{iI}^{\text{int}}(t)=2\pi\int\!\!\int_S (B_I)_{ki}^{T}\sigma_k\,r\,dr\,dz \ \text{for}\ k=1,\cdots,4,i=1,2\ \text{and}\ I=1,\cdots,3 \tag{5}$$

$$f_{iI}^{\text{ext}}(t)=2\pi\int_\Gamma N_I t_i\,r\,d\Gamma \ \text{for}\ (i=1,2),(I=1,\cdots,n_3) \tag{6}$$

where δ_{ij} and ρ in Eq. (4) and t_i in Eq. (6) are Kronecker's delta, density and prescribed traction, respectively, and the integrals in Eqs. (4) and (5) is the surface integral and the one in Eq. (6) is line integral. The Eqs. (4) and (6) are computed by explicit integration and Eq. (5) by standard 3-point Gaussian quadrature[5], respectively. Thus, with the application of new-mark β method[6] for time discretization, nodal acceleration, velocity and displacement as well as stresses and strains are updated.

2.2 Modeling of tensile fracture

In the axisymmetric problem, there are 3 principal directions, i.e. one component is in r-θ plane and other two components are in r-z plane. Thus, the number of corresponding principal stresses is 3, and therefore fractures in 3 directions have to be considered. The treatment of fracturing in r-z plane and r-θ plane is individually described as follows.

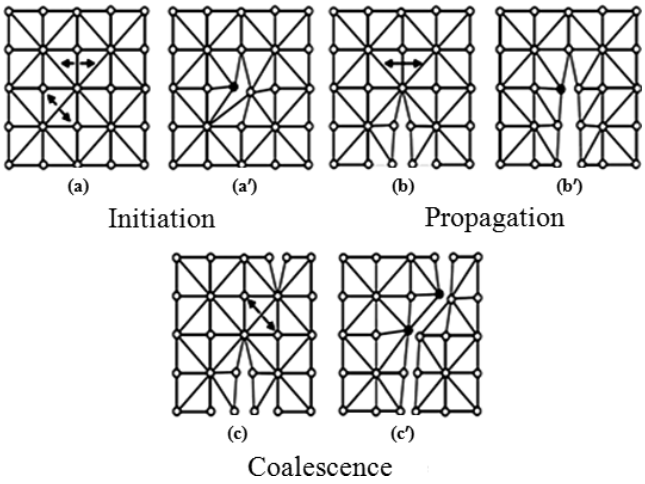

Figure 2 Remeshing procedures for the tensile fracture.

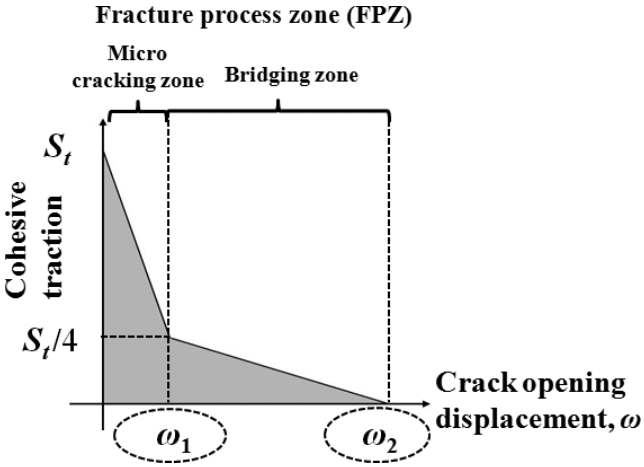

Figure 3 Tensile softening curves for the FPZ.

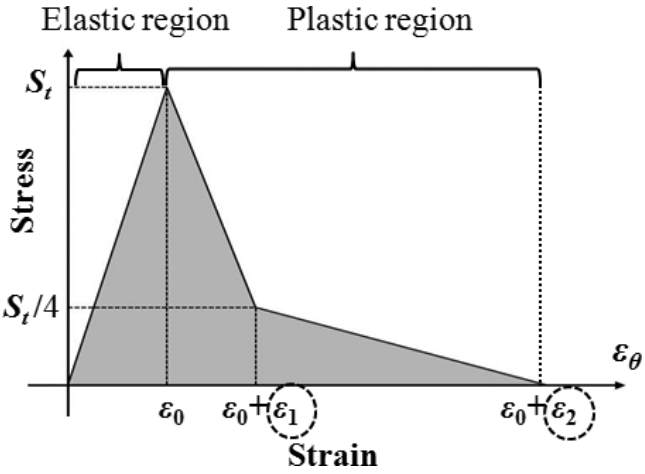

Figure 4 Tensile softening curve in $r-\theta$ plane.

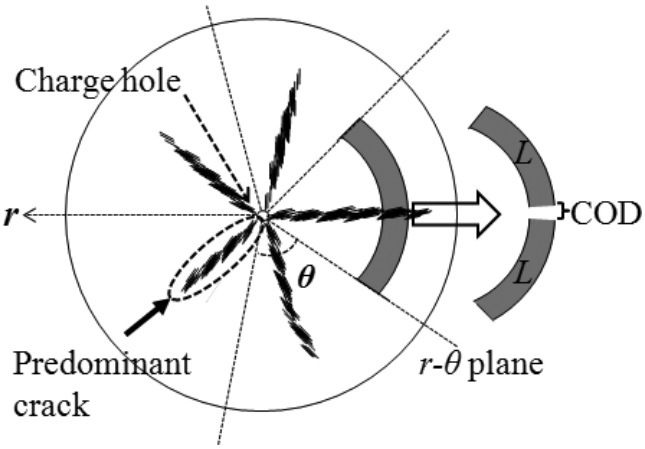

Figure 5 An interpretation of crack propagation in $r-\theta$ plane.

2.2.1 Tensile fracture in r-z plane

For the tensile fracture in r-z plane, we used inter element cracking method[2] applied by Kaneko et al. as shown in Figure 2 where the crack initiation, propagation and coalescence were expressed by element separations when the induced stress normally acting on element-boundary exceeded given tensile strength of the boundary. Once the crack was initiated, non-linear crack opening behavior due to the existence of fracture process zone (FPZ) near the crack tip was considered, and the bi-linear model of cohesive law characterized by cohesive traction and crack opening displacement (COD) shown in Figure 3 was used.

2.2.2 Tensile fracture in r-θ plane

Tensile fracture in r-θ plane was also taken into account in the axisymmetric problem. However, because u_θ is 0 in this class of problem, the cohesive law in Figure 3 cannot apply directly. Alternatively, we used stress-strain relation in each element to express the decohesion of crack surfaces in r-θ plane as shown in Figure 4. In this approach, stress (σ_θ)-strain (ε_θ) relation was expressed by linear elastic behavior when the induced stress level was below the given tensile strength, then, after the stress exceeded the given tensile strength, the stress-strain relation corresponding to the decohesion process characterized by bi-linear model of cohesive law was used instead of COD. To reasonably evaluate strains, ε_1 and ε_2, in the decohesion process, we refer to a fracture pattern obtained by the 2 dimensional Dynamic Fracture Process Analysis in the cross section of Figure 1 (a) (r-θ plane) as shown in Figure 5. The 2 dimensional DFPA was conducted under plane strain condition. We can observe the predominant cracks.[3] Based on this, we equally divided the domain to subdomains each of which included one predominant crack, and we approximately determined crack opening strain (COS) by the ratio of COD to arch length L of subdomains shown in Figure 5. For the computation of L, r at the centroid of each element was used.

$$L = \frac{2\pi r}{n} \tag{7}$$

where n is number of the dominant cracks. Following this concept, we computed ε_1 and ε_2 by COD_1/L and COD_2/L, respectively.

2.2.3 Modeling of heterogeneous material

As an extension of previous works[2], microscopic tensile strength distribution in the material was expressed by Weibull's distribution characterized by coefficient of uniformity, m. However, the concept of heterogeneity in the axisymmetric problem showed a contradiction in that

the axisymmetry with respect to z axis required the strength distribution to be axisymmetric in the r-z planes for each θ. We show in the next section (see 3.2.3) that resultant fracture pattern under $m = 30$, i.e. heterogeneous condition, become relatively homogeneous.

3. DFPA under axisymmetric condition

3.1 Model description

In Figure 6 (a), a cylindrical concrete having a cylindrical charge hole is shown with the size of model. The consideration of axisymmetry with respect to the axial direction of charge hole leads to the FEM mesh shown in Figure 6 (b). Each element size was set to be small enough to avoid the mesh dependency of crack path. The analysis model has one free face only upper part. The total element number and initial total nodal number were 69364 and 35000, respectively. The physical properties of concrete used in the analysis are shown in Table 1. To model the borehole pressure the following pressure function was applied to the surface of the charge hole as shown in Figure 6 (b):

$$P(t) = P_0\{1 - \exp(-\alpha t)\} \tag{8}$$

Table 1 Physical properties of concrete.

Properties	Value
Density [kg·m^{-3}].	2200
P−wave velocity [m·s^{-1}].	4000
S−wave velocity [m·s^{-1}].	2450
Young's modulus [GPa].	31.7
Poisson's ratio	0.2
Mean tensile strength [MPa].	6
Fracture energy [Pa m].	96

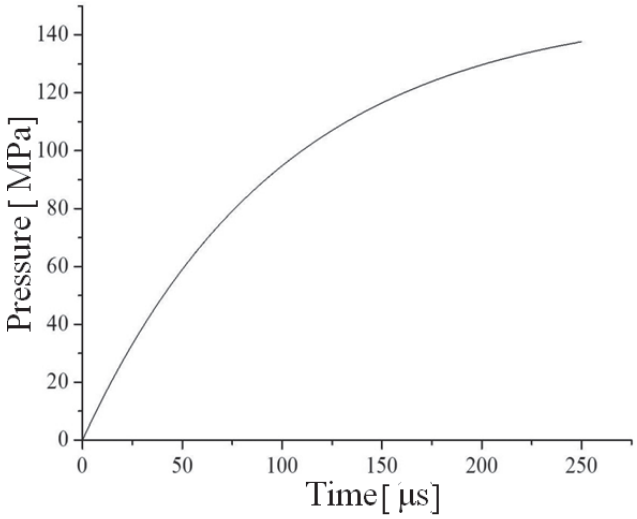

Figure 7 Pressure-time curve for applied pressure waveform.

where $P(t)$ is the pressure at time t, P_0 donates the peak pressure value, and α is constant. Figure 7 shows the applied pressure wave form with the rise time being 10 μs when $\alpha = 10^4$.

3.2 Fracture process in rock-like material with a cylindrical charge hole

3.2.1 DFPA result

In Figure 8, the result of fracture process under $m = 30$ and $n = 5$ from time $t = 0$ to 250 μs is shown where solid black lines are tensile fractures initiated and extended in r-z plane (r-z fractures), and red colored regions correspond to the tensile fractures due to r-θ plane (r-θ fractures). Around $t = 100$ μs, the r-z and r-θ fractures initiated from the side wall of the charge hole were observed. The r-z fractures extending obliquely

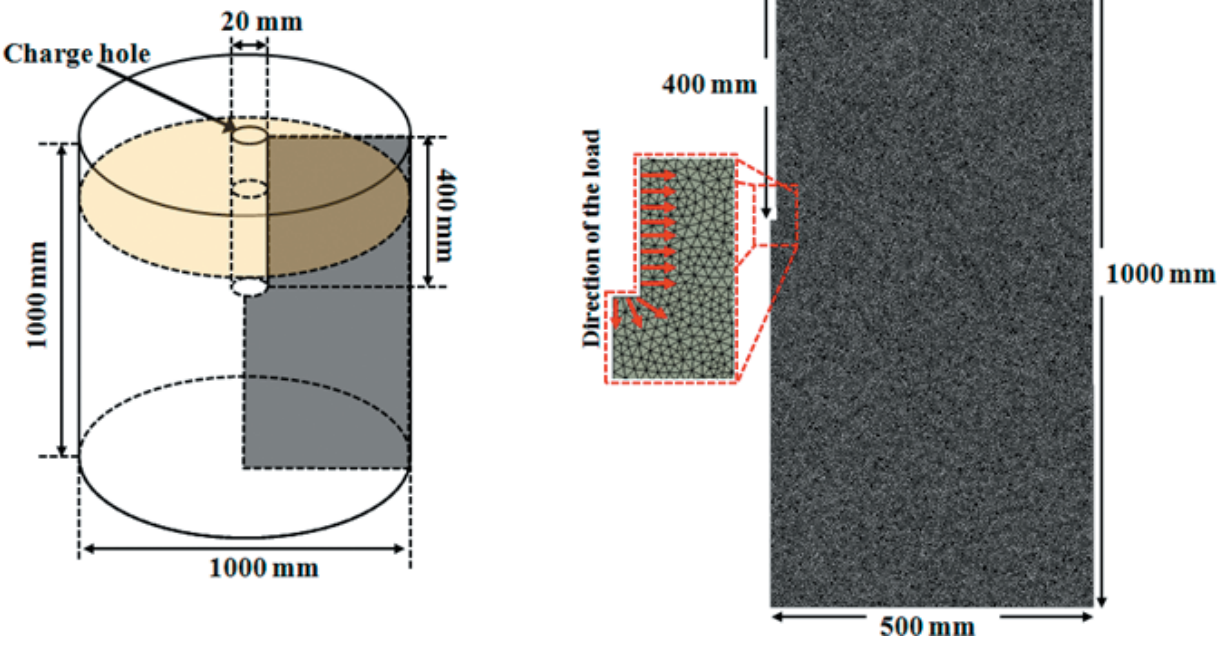

(a) Cylindrical specimen (b) Finite element layout

Figure 6 Description of numerical model.

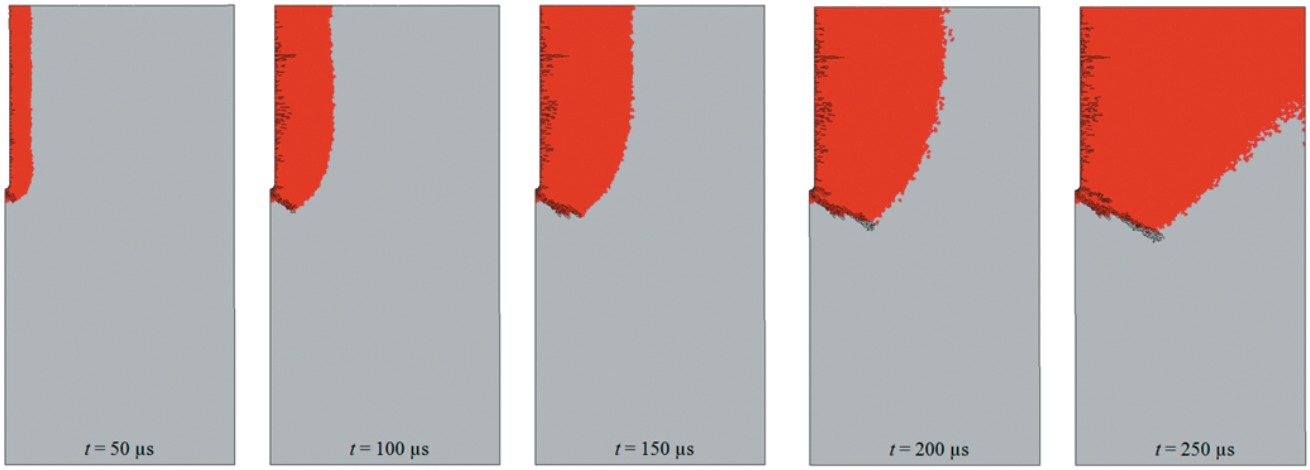

Figure 8 Result of fracture process ($m = 30, n = 5$).

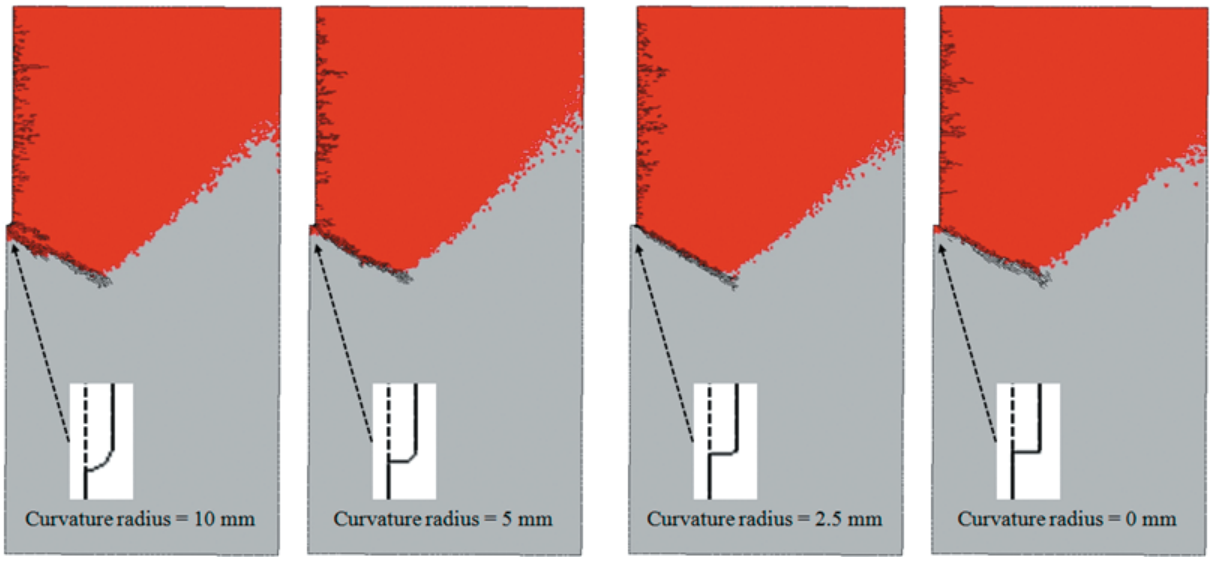

Figure 9 Influence of curvature radius of charge hole on resultant fracture pattern ($m = 30, n = 5$).

downward from the bottom of the charge hole were also found. While the minor extensions of the r-z fractures from the side wall of charge hole was found, the major extension of the oblique r-z fractures and r-θ fractures were found where the r-θ fractures only occurred above the oblique r-z fractures and the most significant r-θ fractures were found on the upper surface of the model.

3.2.2 Influence of the bottom shape of charge hole

Because the existence of corner around the bottom of the charge hole could induce stress concentration, we investigated the effect of bottom shape of the charge hole on the resultant fracture pattern. For this purpose, we considered four models similar to the one in Figure 6 (b) where only bottom shapes of charge hole were changed in terms of curvature radii, 10 mm, 5 mm, 2.5 mm and 0, respectively, in each model. In Figure 9, the resultant fracture patterns for the four models are shown corresponding to $t = 250$ μs. These results show that almost same fracture patterns were obtained and thus the oblique r-z fracture from the bottom of charge hole was initiated irrespective of considered curvature radii.

3.2.3 Influence of heterogeneity

In Figure 10, the resultant fracture patterns for the cases of $m = 30$, 10 and 5 under the same model geometry are shown corresponding to $t = 250$ μs. These results show that quite similar fracture patterns were obtained and thus the influence of heterogeneity has minor role on the fracture pattern in the r-z planes.

4. Discussion

Based on the results obtained in Subsection 3.2, the general resultant fracture pattern could become the one shown in Figure 11 (a) consisting of predominant r-θ fractures from the wall and oblique r-z fractures from the bottom of charge hole. Considering that the assumption of decohesion in r-θ fractures was made based on the propagation of predominant cracks from the charge hole, we can expect the 3-D fracture pattern to be the one shown in Figure 11 (b) where the r-θ fractures become 5 predominant radial cracks shown in red color and the r-z fractures become the conical crack shown in black color. The result obtained here shows good agreement with usually observed in rock splitting. Thus proposed method can be useful for the simulation of fracture process having

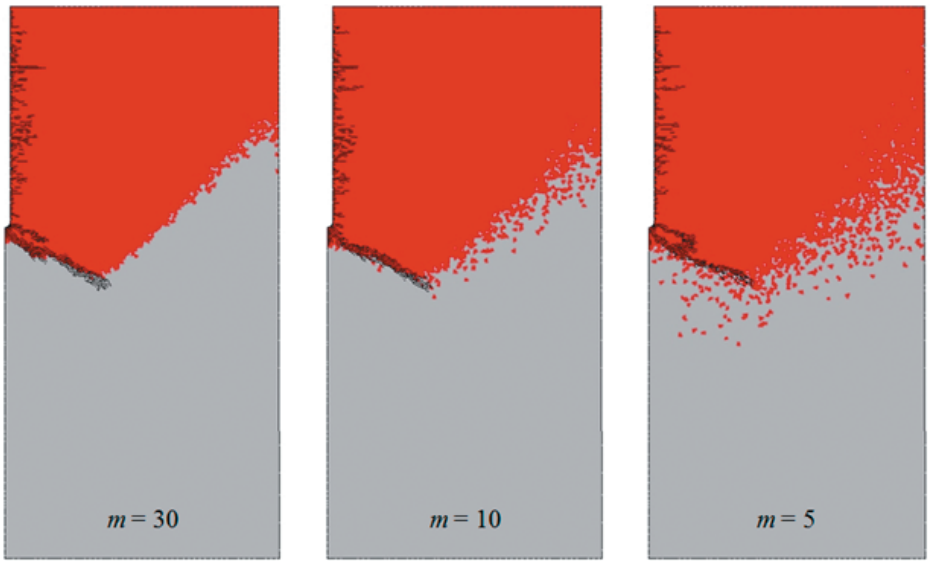

Figure10 Influence of heterogeneity on resultant fracture pattern ($n = 5$).

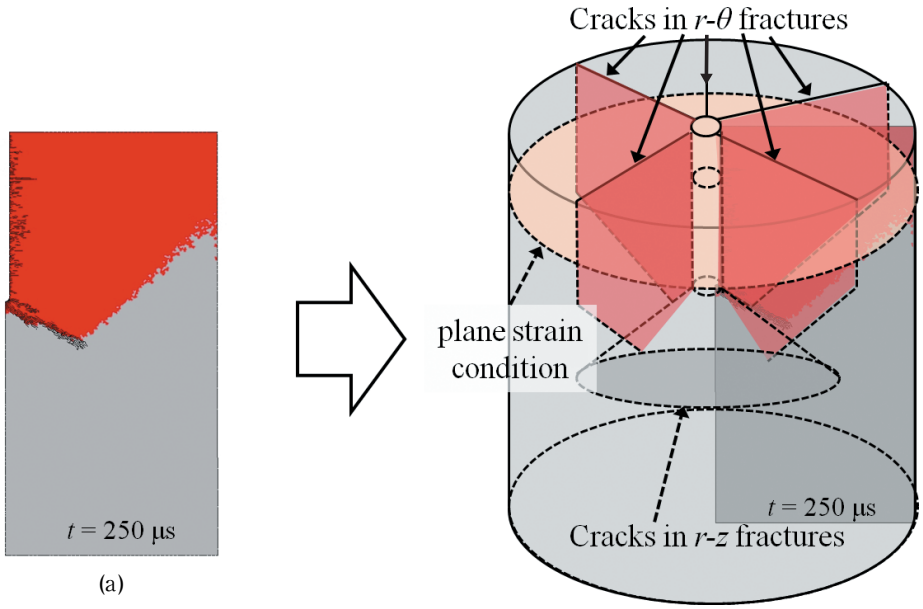

(a) (b)

Figure11 Resultant fracture pattern ($t = 250\ \mu s$).

geometrical axisymmetry.

We additionally compared the fracture processes obtained from plane strain and axisymmetric conditions assuming the same applied load in Eq. (8) and physical properties in Table 1. The result is shown in Figure 12 where one of predominant cracks under plane condition shown in black color is compared to crack propagation obtained from the axisymmetric analysis with the red being fractured and unfractured regions, respectively. The comparison of both analyses shows good agreement in the r-θ fracture propagation velocity. Therefore, this result shows the validity of the proposed method and the axisymmetric analysis could give the insight for the range in which plane strain condition is applicable.

5. Conclusion

We developed a numerical simulation method to simulate the dynamic fracture process in rock-like materials for axisymmetric problems based on finite element method (FEM). This paper described the applied methodology and investigated the validity of the method.

In the proposed method, the conical crack pattern formed from the bottom of charge hole as well as predominant cracks radially extending from the charge hole were successfully simulated. Additionally, the proposed method gave similar fracture patterns compared to those obtained by using previous approach based on the plane strain condition, which shows the validity of the proposed method. In the future work, experiment result of concrete pile top problems can be investigated by the proposed method[7].

Acknowledgments

This work was supported partially by the Technology Innovation Program (2011T100200108) funded by the Ministry of Knowledge Economy (MKE) of Korea. The

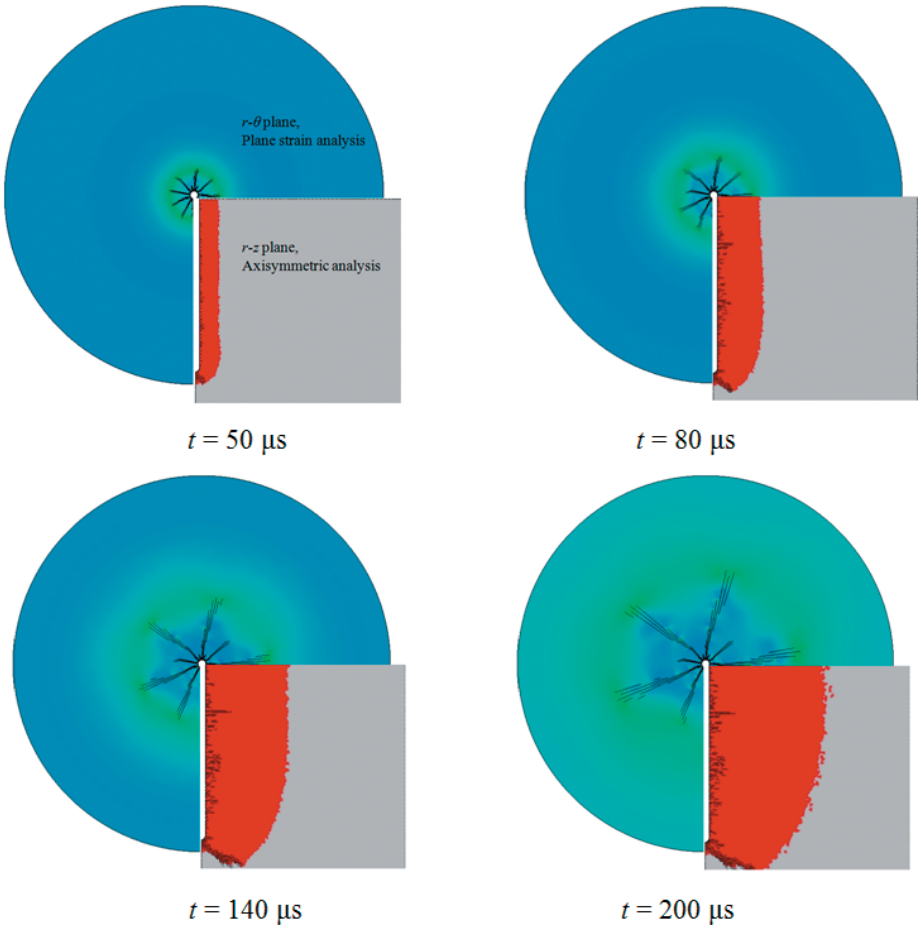

Figure12 Comparison of result in axisymmetric problem with that in plane strain condition.

authors wish to thank Y. Nakamura for his helpful discussion.

References

1) K. Sassa and I. Ito, J. Soc. Mater. Sci. Japan, 21, 123−129, (1972) (in Japanese)
2) K. Kaneko, Y. Matsunaga and M. Yamamoto, Kayaku Gakkaishi (Sci. Tech. Energetic Materials), 56, 207−215, (1995) (in Japanese)
3) S. H. Cho and K. Kaneko, Int. J. Rock mech Min. Sci., 41, 771−784, (2004)
4) T. Belytschko, W. K. Liu and B. Moran, "Nonlinear Finite Elements for Continua and Structures", 622−623, John Wiley & Sons, (2000)
5) G. R. Cowper, lnt. J. Numer. Meth. Eng., 7, 405−408, (1973)
6) N. M. Newmark, J. Eng. Mech. Div. 85, 67−94, (1959)
7) H. M. Kim, S. H. Cho, J. R. Ahn, Y. Nakamura, K. Masatoshi, K. Kaneko, D. Fukuda, K. Moriya, S. K. Kim and C. G. Suk, International Conference of Asian-Pacific Symposium on Blasting Techniques, Xiamen in China, 297−300, (2011)